Two-photon laser excitation of trapped ^{232}Th$^+$ ions via the 402-nm resonance line

O. A. Herrera-Sancho, M. V. Okhapkin, K. Zimmermann, Chr. Tamm, and E. Peik[*]

Physikalisch-Technische Bundesanstalt, Bundesallee 100, 38116 Braunschweig, Germany

A. V. Taichenachev and V. I. Yudin

Institute of Laser Physics, Siberian Branch of RAS, Novosibirsk 630090, Russia, and
Novosibirsk State University, Novosibirsk 630090, Russia

P. Głowacki

Poznań University of Technology, 60-965 Poznań, Poland

Experiments on one- and two-photon laser excitation of ^{232}Th$^+$ ions in a radio-frequency ion trap are reported. As the first excitation step, the strongest resonance line at 402 nm from the $(6d^27s)J = 3/2$ ground state to the $(6d7s7p)J = 5/2$ state at 24874 cm^{-1} is driven by radiation from an extended-cavity diode laser. Spontaneous decay of the intermediate state populates a number of low-lying metastable states, thus limiting the excited state population and fluorescence signal obtainable with continuous laser excitation. We study the collisional quenching efficiency of helium, argon, and nitrogen buffer gases, and the effect of repumping laser excitation from the three lowest-lying metastable levels. The experimental results are compared with a four-level rate equation model, which allows us to deduce quenching rates for these buffer gases. Using laser radiation at 399 nm for the second step, we demonstrate two-photon excitation to the state at 49 960 cm^{-1}, among the highest-lying classified levels of Th$^+$. This is of interest as a test case for the search for higher-lying levels in the range above 55 000 cm^{-1} which can resonantly enhance the excitation of the ^{229}Th$^+$ nuclear resonance through an inverse two-photon electronic bridge process.

PACS number(s): 32.50.+d, 42.62.Fi, 37.10.Ty

I. INTRODUCTION

It has been inferred from γ spectroscopy of ^{229}Th that this nucleus possesses an isomeric state at an energy of only a few eV above the ground state, establishing the lowest excitation energy that is known in nuclear physics. The most recent experimental value for the ^{229}Th isomer energy is 7.8(5) eV [1,2]. This system has stimulated a number of proposals for studies of the effects of atomic electrons on the nuclear transition (see Refs. [3,4] and references therein). These can be expected to be especially pronounced here because of the matching of the nuclear and electronic excitation energies. The radiative decay of the isomeric state can be strongly enhanced in a so-called electronic bridge process where the nucleus excites the electron shell and a photon is finally emitted in an electronic transition. Vice versa, in an inverse electronic bridge process, laser excitation of the nucleus can be more efficient by making use of an electronic excitation that will resonantly couple to the nuclear moments.

Since the nuclear transition frequency in ^{229}Th is accessible by frequency upconversion of narrow-bandwidth laser sources and since it is less sensitive to external perturbations than transition frequencies of the electron shell, we have proposed it as the basis of an optical nuclear clock of high precision [5]. Experiments toward this goal are now pursued with different approaches [6,7]. Up to now, the large uncertainty of the nuclear transition frequency and its location in the vacuum-ultraviolet range has prevented the observation of excitation or decay of the isomeric state of ^{229}Th by means of optical spectroscopy. As a technique to achieve resonant excitation of the ^{229}Th nucleus with the use of conventional laser sources, we have proposed a two-photon inverse electronic bridge process in singly ionized ^{229}Th [8].

The electronic energy level system of Th$^+$ is very complex and is well known only up to an excitation energy of about 7 eV. The classified energy levels belong to the lowest 15 configurations of the three valence electrons. More than 400 energy levels have been identified [9] and the wavelengths of about 14 000 lines are tabulated [10]. Recent relativistic Hartree-Fock calculations indicate an exponential increase of the energy level density toward the ionization energy of 11.9 eV [11].

While the high density of electronic energy levels in Th$^+$ increases the probability for a strong resonance enhancement of electronic bridge processes leading to excitation of the ^{229}Th nucleus, it also poses an experimental problem: Laser excitation of an ensemble of atoms from the ground state to a definite excited state is often inefficient for a multilevel system such as Th$^+$ because spontaneous decay leads to the accumulation of population in metastable levels that are decoupled from the laser. If the number of metastable levels is not too high, additional repumper lasers may be applied for reexcitation from each of those states. Otherwise, atoms in metastable states can be returned to the ground state by inelastic quenching collisions with a buffer gas. The latter approach has already been utilized for laser spectroscopy of Th$^+$ ions: In order to determine the nuclear charge radii of the isotopes ^{227}Th to ^{230}Th and ^{232}Th, isotope shifts and hyperfine splittings have been recorded in one- and two-photon laser excitation to levels at 17 122 and 34 544 cm^{-1} using Th$^+$ ions in a radio-frequency trap in the presence of helium and hydrogen buffer gases [12,13].

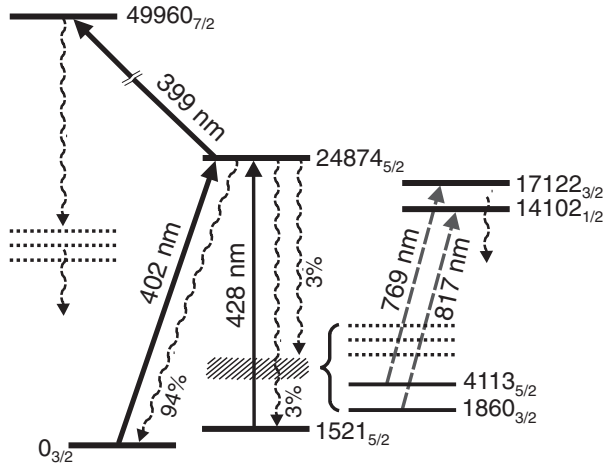[*]Corresponding author: ekkehard.peik@ptb.de

FIG. 1. Partial level scheme of the thorium ion Th$^+$ showing the main resonance transitions studied in this work and the lowest-lying metastable levels. The hatched area corresponds to a manifold of 11 metastable states which is shown in more detail in the right-hand side of the figure. The level energies are given in cm^{-1} and the subscript denotes the total angular momentum. For the 24 874$_{5/2}$ level the spontaneous-decay branching fractions are indicated as given in Ref. [14].

Here we present experiments on one- and two-photon laser excitation of trapped Th$^+$ ions, aimed at an investigation of the electronic energy level system in the range around 7–8 eV and toward the excitation of the ^{229}Th nuclear resonance by an inverse two-photon electronic bridge process. In particular, we investigate excitation of the strongest tabulated line of the Th$^+$ emission spectrum at 402 nm which connects the $(6d^27s)J = 3/2$ ground state with the $(6d7s7p)J = 5/2$ state at 24 874 cm^{-1} [10]. In the following we label states by their energy in cm^{-1} and their total angular momentum as shown in Fig. 1. Spontaneous decay from the 24 874$_{5/2}$ state leads back to the ground state with a rather high probability but a number of low-lying metastable states [14] are also populated (see Fig. 1). We measured branching ratios of 11 decay channels after laser excitation in a hollow-cathode discharge. With trapped ions, we study the collisional quenching efficiency of helium, argon, and nitrogen buffer gases, and the effect of repumping laser excitation from the three lowest-lying metastable levels. We show that the experimental results are in good agreement with a simple four-level rate equation model. Using laser radiation at 402 and 399 nm, we demonstrate two-photon excitation to the level 49 960$_{7/2}$ via the intermediate 24 874$_{5/2}$ state. The observation of two-photon excitation to this level in ^{232}Th$^+$ is of interest because it serves as a test case for the search for higher-lying levels which can resonantly enhance the excitation of the ^{229}Th$^+$ nucleus through an electronic bridge process as pointed out above.

II. EXPERIMENTAL SETUP

The experiment employs a linear radio-frequency (rf) trap of 160 mm in total length (see Fig. 2). The trap electrodes are machined from a CuBe alloy and are divided along their length into three sections which are held at different dc potentials. For ion loading, a metallic ^{232}Th sample is placed between two
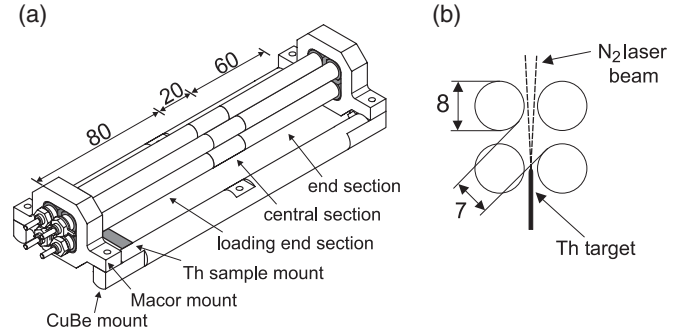

FIG. 2. Schematic of the linear Paul trap used in the experiments (a) and cross section of the trap electrode arrangement, showing the position of the Th sample used for ion loading by N$_2$ laser ablation (b). Dimensions are in millimeters.

electrodes near the end of one of the outer sections. Typically a rf trap drive voltage in the range of 0.5–1 kV amplitude at a frequency of 2 MHz is used, corresponding to a Mathieu q parameter in the range of 0.2–0.4 (for a review see Ref. [15]). The end sections are kept at a dc potential of +40 V relative to the central section for axial confinement.

The trap is mounted in a stainless-steel ultrahigh-vacuum chamber that reaches a base pressure in the range of 1×10^{-8} Pa. For collisional cooling and depopulation of metastable Th$^+$ levels by quenching collisions, helium, argon, or nitrogen at a pressure of up to 0.2 Pa is used as a buffer gas. To produce ^{232}Th$^+$ ions by laser ablation, a nitrogen laser emitting 4-ns pulses with an energy of $\approx$100 μJ at a wavelength of 337 nm is focused to a spot size of 100 μm $\times$ 150 μm on a metallic Th target [see Fig. 2(b)]. After five to ten ablation pulses at 0.2-Pa helium buffer gas pressure, more than 10^5 ions are loaded into the trap (for more details see Ref. [16]). With argon and nitrogen buffer gases the same number of trapped ions is obtained with two to five pulses and with one to two pulses, respectively. We observe storage times for Th$^+$ in the range of 300–1000 s, limited by the formation of molecular ions in reactions with the background gas [13,17].

For excitation of the 0$_{3/2}$–24 874$_{5/2}$ transition (see Fig. 1), a continous-wave (cw) extended-cavity diode laser (ECDL) with a maximum output power of 7 mW at 402 nm and a linewidth of less than 1 MHz is used. The 24 874$_{5/2}$–49 960$_{7/2}$ transition is excited by a similar laser system emitting at 399 nm. The metastable 1521$_{5/2}$ level is depleted by a frequency-doubled ECDL producing light at a wavelength of 428 nm (see Fig. 1). The output of these lasers is passed to the trap through polarization-maintaining single-mode fibers in order to clean the beam profiles, thus minimizing light scattering off the trap electrodes. Beam diameters in the trap are $\approx$1 mm. For low-resolution spectroscopy over extended wavelength ranges, a tunable mode-locked Ti:sapphire laser system producing pulses of about 3 ps in duration and at a repetition rate of 90 MHz is used. Its output wavelength can be tuned in the range of 700–900 nm and in the corresponding second- and third-harmonic ranges.

As shown in Fig. 3, the fluorescence emission of the trapped ^{232}Th$^+$ ions is detected with the use of two photomultipliers placed behind a fused-silica collection lens. In order to discriminate between the fluorescence emissions associated
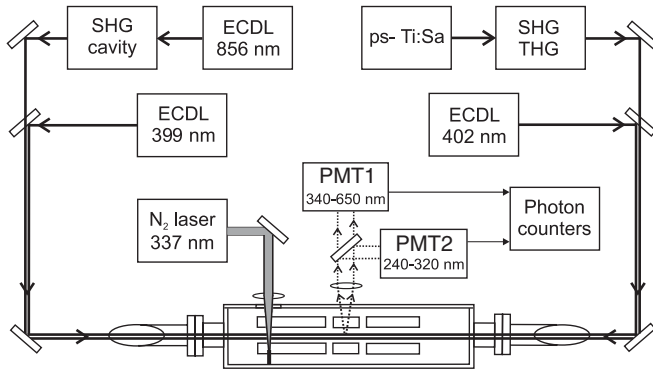
FIG. 3. Experimental arrangement for laser excitation of trapped Th$^+$. Two photomultipliers (PMT) are used for fluorescence detection. A nitrogen laser is used for loading the trap. SHG (THG): Second-harmonic generation (third-harmonic generation). For further details see text.

with one- and two-step excitations, a combination of spectral filters and a dichroic beam splitter separates the spectral sensitivity ranges of the photomultipliers.

III. SINGLE-WAVELENGTH LASER EXCITATION OF ^{232}Th$^+$

In an investigation of possible first excitation steps from the ground state, fluorescence signals of ^{232}Th$^+$ are readily observed by illuminating the trapped ion cloud with output of the picosecond Ti:sapphire laser. A typical excitation spectrum of electric-dipole transitions around 400 nm is shown in Fig. 4(a). In order to compensate variations in signal strength caused by fluctuations of the number of loaded ions, the fluorescence signal registered at each laser wavelength was normalized to the signal resulting from resonant cw diode-laser excitation of the 402-nm transition. Helium was used as a buffer gas at a pressure of $\approx$0.2 Pa. The transitions from the ground state displayed in Fig. 4(a) and their relative strengths are in agreement with the data tabulated in Ref. [9] for the investigated scan range.

The spectrum resulting from 402-nm cw laser excitation is shown in Fig. 4(b). While the wide linewidths in Fig. 4(a) are determined by the spectral width of the employed laser, the linewidth in Fig. 4(b) is determined by Doppler broadening.
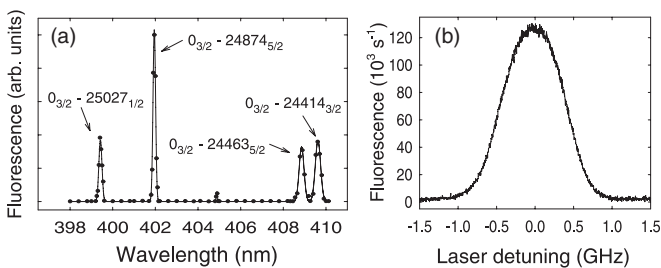

FIG. 4. Excitation spectra of trapped ^{232}Th$^+$ ions, using (a) the second-harmonic output of a mode-locked Ti:sapphire laser and (b) the cw output of an extended-cavity diode laser tuned to the $0_{3/2}$–$24\,874_{5/2}$ transition at 402 nm. In panel (a), the average excitation power is 10 mW and the data points (black dots) are fitted by Lorentzian profiles. In panel (b), the power is 50 μW.

For helium pressures above 0.1 Pa the Doppler width of $\approx$700 MHz (FWHM) indicates that the trapped ions are collisionally cooled to approximately 300 K for motion along the trap axis. With argon and nitrogen buffer gas, cooling to room temperature is achieved at pressures of $\approx$0.2 and $\approx$0.01 Pa, respectively. With these gases at 0.2-Pa pressure, fluorescence signals larger than those obtained with helium are observed, because of more efficient collisional quenching of metastable levels (see below). For cw excitation of the 402-nm transition, the strength of the fluorescence signal is strongly affected by population trapping in metastable levels.

For a quantitative overview on the decay channels of the $24\,874_{5/2}$ level we performed measurements of the fluorescence emission resulting from laser excitation of Th$^+$ ions in a hollow-cathode discharge. The hollow-cathode lamp has a similar construction as described in Refs. [18,19]: The cathode is a 2.5-cm-long copper cylinder with an inner diameter of 6 mm, covered by a thorium foil on the inner wall, and is cooled by liquid nitrogen. The discharge is operated at a current of 40 mA with argon buffer gas at a pressure between 80 and 100 Pa. A 5-mW laser beam from the 402-nm ECDL, resonant with the $0_{3/2}$–$24\,874_{5/2}$ transition, is directed through the cathode. A mirror with a central hole for passage of the laser beam collects the fluorescence light from the center of the cathode onto the entrance slit of a grating monochromator. After passage through the monochromator the light is detected with a photomultiplier and recorded differentially with and without laser excitation, in order to separate the laser-induced fluorescence from emission excited by the discharge. The spectral sensitivities of the monochromator and the photomultiplier are calibrated with a tungsten reference lamp. Since laser stray light would perturb the fluorescence intensity measurement at the wavelength used for excitation, the intensity ratios of the lines at 402, 434, and 482 nm were also measured with laser excitation of the $1521_{5/2}$–$24\,874_{5/2}$ transition at 428 nm. The wide dynamic range of the detection method allowed us to measure relative intensities of 11 emission lines listed in Ref. [9], complementing a previous study that had reported branching fractions for 6 lines [14]. The 2 weakest lines at 812 and 1073 nm were not observed. Table I summarizes the results. Based on the observed reproducibility for different discharge conditions, we attribute a relative uncertainty of about 0.1 to the branching fractions for the weak decay channels. The branching fraction for decay on the resonance line 402 nm back to the ground state of 0.92(3) is in good agreement with the value of 0.94 from Ref. [14] and higher than the value of 0.85 obtained in the analysis in Ref. [20]. Cyclic laser excitation of the 402-nm resonance line in a single Th$^+$ ion can therefore be expected to result in about 15 fluorescence photons before decay into a metastable level occurs.

IV. EFFECTIVE FOUR-LEVEL MODEL FOR COLLISIONAL QUENCHING AND REPUMPING

In order to obtain a simple analytic description, we approximate the Th$^+$ level system up to the $24\,874_{5/2}$ level by the four-level system shown in Fig. 5: the 402-nm transition from the ground state $|1\rangle$ to state $|3\rangle$ is driven with Rabi frequency Ω_1, the metastable state $|2\rangle$ is depleted by 428-nm repumping light with Rabi frequency Ω_2, and the manifold of 11 higher-lying

TABLE I. Branching fractions (BF) for decay of the Th$^+$ level $24\,874_{5/2}$ to various lower-lying metastable states.

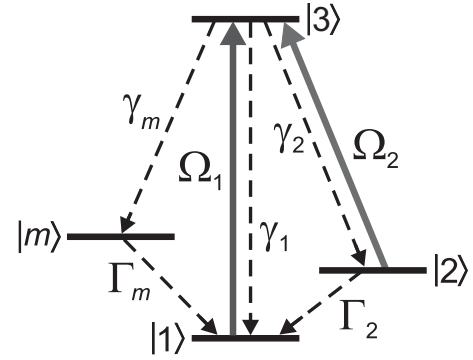| Lower level (cm^{-1})	λ_{air} (nm)	BF (this work)	BF (Ref. [14])
0	401.9	9.2×10^{-1}	9.4×10^{-1}
1521	428.1	3.3×10^{-2}	3×10^{-2}
1860	434.4	2.7×10^{-2}	1×10^{-2}
4013	481.5	3×10^{-5}	–
4146	482.3	7×10^{-3}	1×10^{-2}
7001	559.4	6×10^{-3}	1×10^{-2}
8460	609.1	5×10^{-4}	–
8605	614.5	2×10^{-3}	4×10^{-3}
9061	632.2	2×10^{-4}	–
9711	659.4	4×10^{-4}	–
13250	860.1	4×10^{-5}	–

FIG. 5. Energy level system considered in the rate equation model of Eq. (1). The levels $|1\rangle$, $|3\rangle$, $|2\rangle$, and $|m\rangle$ represent the ground state, the $24\,874_{5/2}$ level, the $1521_{5/2}$ level, and a manifold of 11 metastable states, respectively (cf. Fig. 1).

metastable states is represented by a single level $|m\rangle$. Here we assume that $|m\rangle$ is depleted only by quenching collisions. The excited state $|3\rangle$ radiatively decays into the states $|1\rangle$, $|2\rangle$, and $|m\rangle$ with rates γ_1, γ_2, and γ_m. Their sum, $\gamma = \gamma_1 + \gamma_2 + \gamma_m$, determines the radiative lifetime of the state $|3\rangle$ as $\tau = \frac{1}{\gamma}$. For our analysis we use the experimental lifetime value $\tau = 23$ ns [20]. We assume that $\gamma_1 = b\gamma$ and $\gamma_2 = \gamma_m = (1-b)\frac{\gamma}{2}$, and $b = 0.94$ as the branching fraction for decay to the state $|1\rangle$, because the branching fractions for decay to the $1521_{5/2}$ level and for decay to $|m\rangle$ are approximately equal (see Ref. [14] and Table I). The populations of $|2\rangle$ and $|m\rangle$ can decay to the ground state through quenching collisions with buffer gas and the corresponding rates are denoted by Γ_2 and Γ_m. Neglecting the light-induced coherence between states $|1\rangle$ and $|2\rangle$, the population distribution among the levels can be described by rate equations for the population probabilities p_i ($i = 1, 2, 3, m$). In the steady-state limit the rate equations of the four-level system shown in Fig. 5 can be expressed as

$$-\gamma S_1 p_1 + \Gamma_2 p_2 + \gamma_1 p_3 + \gamma S_1 p_3 + \Gamma_m p_m = 0,$$
$$-\gamma S_2 p_2 - \Gamma_2 p_2 + \gamma_2 p_3 + \gamma S_2 p_3 = 0,$$
$$\gamma S_1 p_1 + \gamma S_2 p_2 - \gamma p_3 - (S_1 + S_2)\gamma p_3 = 0, \quad (1)$$
$$\gamma_m p_3 - \Gamma_m p_m = 0,$$

with the normalization condition $\sum p_i = 1$. Here S_j ($j = 1, 2$) are the saturation parameters for the transitions $|j\rangle$–$|3\rangle$. Assuming thermalization of velocities due to both velocity-changing collisions and interaction with the trap potential, and vanishing detunings from the transitions $|j\rangle$–$|3\rangle$, we approximate the optical pumping rates as

$$\gamma S_j \approx 2\sqrt{\pi} \frac{\Omega_j'^2}{kv}, \quad (2)$$

where $kv \approx 2\pi \times 360$ MHz is the Doppler width. For linearly polarized laser fields, the effective Rabi frequencies Ω_j' are obtained by averaging over the Zeeman sublevels:

$$\Omega_j'^2 = \frac{(2J_3 + 1)}{3(2J_j + 1)} \Omega_j^2, \quad (3)$$

where J_j is the total angular momentum of the level $|j\rangle$.

Solving the rate equations, the population of state $|3\rangle$ is

$$p_3 = [2G_2 G_m S_1 + 2G_m S_1 S_2]\{2G_2 G_m$$
$$+ [(1-b)(G_2 + G_m) + 4G_2 G_m]S_1 + [(1+b)G_m$$
$$+ 2G_2 G_m]S_2 + [(1-b) + 6G_m]S_1 S_2\}^{-1}, \quad (4)$$

where $G_k = \Gamma_k/\gamma$ ($k = 2, m$). The observed fluorescence rate is proportional to p_3. If both optical excitations $|j\rangle$–$|3\rangle$ saturate the corresponding transitions, $S_1 \gg (1+b)G_2/(1-b)$ and $S_2 \gg (G_2 + G_m)$, the fluorescence rate is limited by the quenching relaxation of the state $|m\rangle$:

$$p_3 \approx \frac{2G_m}{1-b}. \quad (5)$$

In the absence of the repumping field ($S_2 = 0$), level $|2\rangle$ is depleted only by quenching collisions. In this case the fluorescence rate is reduced and can be expressed as follows:

$$p_3 \approx \frac{2G_m}{1-b} \frac{G_2}{G_2 + G_m}. \quad (6)$$

According to Eqs. (5) and (6), the fluorescence enhancement factor g due to repumping from level $|2\rangle$ obtained in the limit of high 402- and 428-nm laser powers is given by $g = 1 + \Gamma_m/\Gamma_2$.

V. QUENCHING RATES AND POPULATION OF THE $24874_{5/2}$ LEVEL

Based on the results of the four-level model description and using repumping excitation from the $1521_{5/2}$ level, we determine the collisional quenching rates of this level and of the manifold of the other metastable levels which are populated during continuous excitation of the 402-nm $0_{3/2}$–$24\,874_{5/2}$ transition. Quenching rate coefficients are determined for helium, argon, and nitrogen buffer gases. In order to find conditions which minimize the population of metastable levels and thus maximize the population of the $24\,874_{5/2}$ state, we also investigate the effect of additional repumping excitation from the manifold of the levels above the $1521_{5/2}$ level, which are described as the effective level $|m\rangle$ in the model calculation (see Fig. 5).

The data points in Fig. 6(a) show the relative increase in the fluorescence signal at 402 nm which results from the
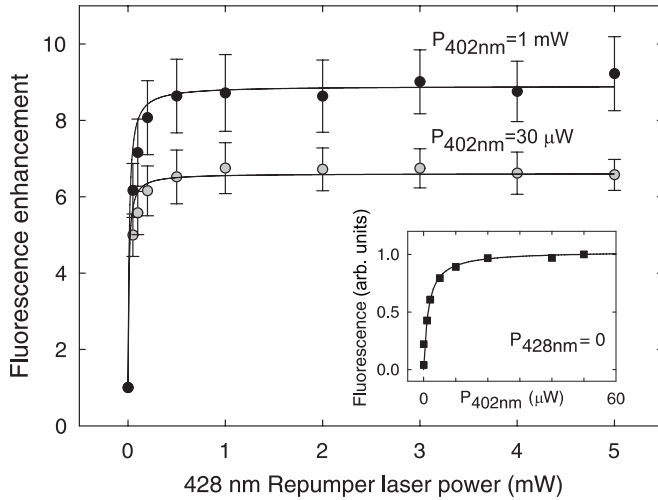
FIG. 6. Fluorescence signal of trapped Th^+ ions resulting from resonant laser excitation of the 402-nm $0_{3/2}$–$24\,874_{5/2}$ transition, showing the fluorescence enhancement due to repumping excitation at 428 nm for two settings of 402-nm excitation power (solid and open circles) with helium buffer gas. The data points are normalized to the fluorescence levels observed without 428-nm excitation. The lines correspond to solutions of Eq. (4) using excitation and quenching rate parameters corresponding to the conditions of the experiment (see text). The data points in the inset show the variation of the fluorescence signal with 402-nm laser power observed in the absence of 428-nm excitation. The solid line corresponds to the solution of Eq. (4) using the same parameters as in the main figure.

repumping excitation of the $1521_{5/2}$–$24\,874_{5/2}$ transition at 428 nm. Helium was used as a buffer gas at 0.2-Pa pressure. The data were obtained for two settings of 402-nm laser power which differ by more than 1 order of magnitude. It appears that the fluorescence signal is enhanced by up to a factor of 9 at a repumping laser power above 0.5 mW. The enhancement is less pronounced if the 402-nm power is reduced. If argon is used at the same pressure, the repumping excitation at 428 nm leads to a maximum fluorescence enhancement of $g \approx 2$, and using nitrogen, only a negligible fluorescence enhancement is observed. At variance with helium, with argon and nitrogen buffer gases a weak fluorescence signal is also observed if the $^{232}Th^+$ ions are illuminated only by the 428-nm light without excitation at 402 nm. This observation indicates that the $1521_{5/2}$ level can be populated by Th^+-Ar and Th^+-N_2 collisions.

Using the experimental data for high and low 402-nm excitation power shown in Fig. 6 together with the calculated optical excitation rates and the natural lifetime and spontaneous-decay branching fractions of the $24\,874_{5/2}$ state from Ref. [14] (see Table I), we find a good agreement between the observed fluorescence enhancement factor g and the predictions of Eq. (4) with $\Gamma_2 = 20$ s^{-1} for helium. As shown in Table II, we find in a similar way $\Gamma_2 = 1.5 \times 10^3$ s^{-1} for argon and $\Gamma_2 = 5.0 \times 10^4$ s^{-1} for nitrogen, at 0.2-Pa pressure for all gases. Using the branching fraction $b = 0.92$ measured in our experiments (see Table I), we obtain slightly higher quenching rates (for example, for helium, $\Gamma_2 = 25$ s^{-1}). The diatomic buffer gas N_2 yields much higher quenching efficiency than the noble gases. A similar behavior is known

TABLE II. Quenching rates Γ_2 for different buffer gases at 0.2-Pa pressure and estimated population p_3 in the state $|3\rangle$ without and with repumping at 428 nm.

Buffer gas	Γ_2 (s^{-1})	p_3 (without 428 nm)	p_3 (with 428 nm)
Helium	20	1.5×10^{-5}	1.2×10^{-4}
Argon	1.5×10^3	5.0×10^{-4}	1.0×10^{-3}
Nitrogen	5.0×10^4	5.0×10^{-3}	

for the collisional quenching rates of the metastable D levels in alkali-metal-like ions [21,22].

The inset of Fig. 6 shows that Eq. (4) also accurately describes the observed saturation behavior of the 402-nm excitation without 428-nm repumping. In this case, the population of the $1521_{5/2}$ state reduces the effective saturation power for excitation of the 402-nm transition to a few microwatts corresponding to an intensity of ≈ 0.3 mW/cm^2, i.e., 2 orders of magnitude below the saturation intensity for the two-level system $0_{3/2}$–$24\,874_{5/2}$. With helium buffer gas, the observed variation of g with pressure points to a linear pressure dependence of the rate Γ_2 and to a less than proportional variation of Γ_m with pressure. At a lower helium pressure of 0.02 Pa, the 428-nm repumping excitation enhances the fluorescence signal by $g \sim 20$.

Using time-separated pulsed 402- and 428-mn excitation we obtain a direct measurement of the quenching rate Γ_2 of the $1521_{5/2}$ level. The $1521_{5/2}$ level is populated via the $24\,874_{5/2}$ state during a 2-ms pulse of the ECDL at 402 nm. After a variable time delay, the remaining population of the $1521_{5/2}$ level is determined by applying a pulse from the 428-nm ECDL and recording the time-integrated fluorescence signal at 402 nm. A similar method was used in Refs. [21,22]. We observe an exponential decay of the fluorescence signal as a function of the time delay between the 402- and 428-nm excitation and a linear dependence of the decay rate on the He pressure of 63(3) s^{-1} Pa^{-1}. For a pressure of 0.2 Pa, this results in $\Gamma_2 = 13(2)$ s^{-1}, in agreement with the value derived above with Eq. (4) from the data for continuous excitation.

In order to maximize the efficiency of laser excitation to the $24\,874_{5/2}$ level, we investigated extended repumping schemes where in addition to the $1521_{5/2}$ level also higher-lying metastable levels were depleted by laser excitation (see Fig. 1). The output wavelength of the pulsed Ti:sapphire laser (see Sec. II) was tuned to suitable repumping transitions for the six lowest metastable levels above the $1521_{5/2}$ level that were populated by spontaneous decay from the $24\,874_{5/2}$ level. For helium buffer gas at 0.2 Pa, a fluorescence enhancement of approximately a factor of 3 is observed for excitation of the $4113_{5/2}$–$17\,122_{3/2}$ transition and for a number of other transitions originating from the $4113_{5/2}$ level. Excitation from higher-lying metastable levels does not lead to any significant increase in the fluorescence signal. The depletion of the $1860_{3/2}$ level increases the fluorescence signal only if there is no repumping excitation from the $1521_{5/2}$ level. This can be explained by a collision-induced population transfer between the $1521_{5/2}$ and $1860_{3/2}$ levels whose energy difference is comparable to the kinetic energy of the buffer gas atoms. With argon or nitrogen buffer gas, repumping from the energy

levels above the $1521_{5/2}$ level does not result in any significant fluorescence enhancement.

Table II shows the inferred effective quenching rates together with the calculated population probability of the $24\,874_{5/2}$ level under cw laser excitation for the three gases used in our investigations. For helium, additional repumping from the $4113_{5/2}$ level yields a maximum population of 3.6×10^{-4} in the $24\,874_{5/2}$ level. For all experimental conditions studied here, population trapping in low-lying metastable levels limits the obtainable population of the $24\,874_{5/2}$ state. In previous experiments with trapped Th^+ ions, molecular hydrogen and helium buffer gas were compared and hydrogen was found to produce ≈ 100 times higher fluorescence signal at the same pressure [13]. In our experiment, nitrogen shows an even stronger quenching efficiency. From the maximum 402-nm fluorescence signal obtained with nitrogen we deduce that more than 100 photons/s per ion are detected, providing efficient diagnostics of the trapped ions on the time scale expected for the decay of the ^{229}Th isomeric state [23]. While nitrogen produces the highest fluorescence rate and the most efficient collisional cooling, the noble gases offer the advantage that they can be purified more efficiently using getter materials and cryogenic traps and therefore permit longer storage times for Th^+.

With the use of pulsed optical excitation, even without repumping excitation a significantly higher population in the $24\,874_{5/2}$ level can be achieved over times that are short compared to $1/\Gamma_2$ and $1/\Gamma_m$. This could be demonstrated by using an acousto-optical modulator (AOM) to switch on the 402-nm excitation repeatedly with a rise time of approximately 1 μs after dark periods that are long compared to $1/\Gamma_2$. The resulting initial fluorescence intensity is more than 30 times larger than the steady-state value obtained with 402-nm cw excitation and helium buffer gas. The decay of the fluorescence signal to the level corresponding to cw excitation was dominated by two time constants in the range of a few hundred ns and 1 ms. The longer time constant might reflect the collision-induced population transfer between the various metastable levels (see above). The observed fast time constant cannot be directly associated with the spontaneous-decay rates to metastable levels because also transit-time and saturation effects and the rise time of the AOM shutter are expected to strongly affect the temporal variation of the fluorescence signal on this time scale.

VI. TWO-PHOTON LASER EXCITATION OF TRAPPED $^{232}\text{Th}^+$ IONS

The level $49\,960_{7/2}$ shown in Fig. 1 is one of the highest-lying tabulated energy levels that can be excited by an electric dipole transition from the $24\,874_{5/2}$ state. The radiative lifetime of this level appears to be unknown. Apart from the 399-nm transition to the $24\,874_{5/2}$ level, there are 17 tabulated decay channels to other levels [9]. The energy of the $49\,960_{7/2}$ state corresponds to 6.2 eV, which is close to the range of the expected isomeric excitation energy of $^{229}\text{Th}^+$.

In our experiment, trapped Th^+ ions collisionally cooled by buffer gases at 0.2-Pa pressure are continuously excited by 402-nm radiation tuned to the line center of the $0_{3/2}$–$24\,874_{5/2}$ transition and by 428-nm repumping light. A beam of 399-nm
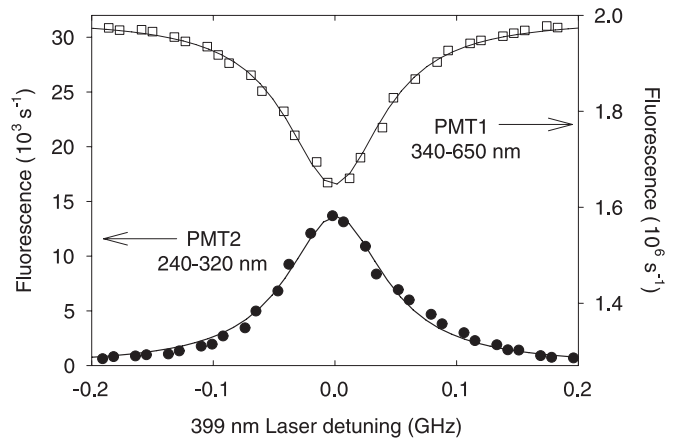

FIG. 7. Two-photon laser excitation spectrum for counterpropagating laser beams, showing fluorescence signals from the upper $49\,960_{7/2}$ level (solid circles) and from the intermediate $24\,874_{7/2}$ state (open squares). Radiation at 402 nm is tuned to the line center of the $0_{3/2}$–$24\,874_{5/2}$ transition and 399-nm light is scanned in the range of the $24\,874_{5/2}$–$49\,960_{7/2}$ transition. The solid lines are fits to a Lorentzian line shape.

light from an ECDL whose frequency is scanned across the $24\,874_{5/2}$–$49\,960_{7/2}$ transition is overlapped co- or counterpropagating with the 402-nm beam. Excitation to the $49\,960_{7/2}$ level is detected by monitoring the fluorescence emission in the wavelength range below 320 nm. Figure 7 shows the two-photon excitation spectrum observed for counterpropagating 402- and 399-nm excitation beams using helium buffer gas at 0.2 Pa. The fluorescence signal observed in the range 340–650 nm, also shown in Fig. 7, indicates the population of the intermediate $24\,874_{5/2}$ level. The resonant reduction of this fluorescence shows that a substantial fraction of ions ($\approx 20\%$ for counterpropagating beams) is transferred from the $0_{3/2}$–$24\,874_{5/2}$ excitation cycle if the $24\,874_{5/2}$–$49\,960_{7/2}$ transition is resonantly excited. This shows that even in the case of the complex level-structure of Th^+, efficient two-photon excitation of highly excited states can be achieved.

Generally, one expects that both stepwise and direct two-photon excitation processes contribute to the population of the $49\,960_{7/2}$ level. With counterpropagating beams, the linewidth of the two-photon resonance is narrower and the fluorescence signal is approximately 1.5 times higher than with copropagating beams (see Fig. 8). In the copropagating case the sub-Doppler resonance populating the $49\,960_{7/2}$ level is formed predominantly by stepwise two-photon excitation, while in the counterpropagating case an additional contribution of direct two-photon excitation appears. A similar feature was observed in a previous investigation on two-photon excitation between lower-lying energy levels of trapped Th^+ ions [13].

In Fig. 8 the experimental data for co- and counterpropagating beams are plotted together with calculated line shapes based on the model presented in Ref. [24]. The homogeneous linewidth of the 402-nm transition was inferred from Doppler-free saturation resonances of the transition at 402 nm. Using nitrogen buffer gas, we here observe a minimum width of 26(2) MHz (FWHM), significantly higher than the natural linewidth of the $24\,874_{5/2}$ state of 7 MHz. Apart from smaller contributions from saturation, collisions, and transit effects, the
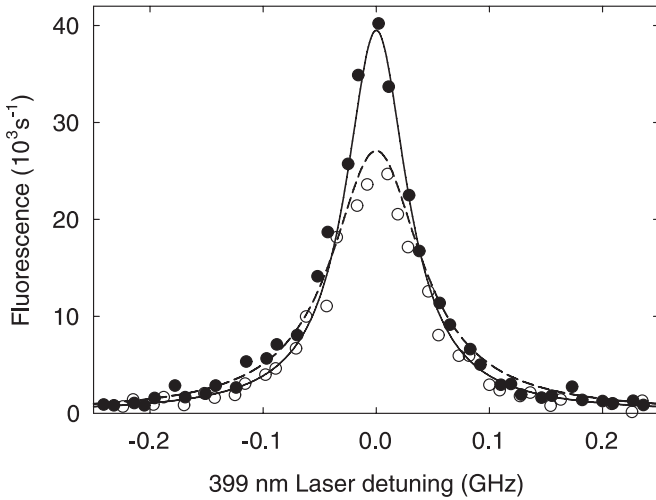
FIG. 8. Fluorescence signal of trapped ^{232}Th$^+$ ions resulting from two-photon laser excitation of the $49\,960_{7/2}$ level. The spectra are detected by monitoring the fluorescence emission in the wavelength range 240–320 nm. Nitrogen at 0.2 Pa is used as a buffer gas. Solid circles: counterpropagating beams; open circles: copropagating beams. The black (counterpropagating beams) and dashed (copropagating beams) lines correspond to calculations based on the model from Ref. [24].

dominant broadening mechanism can likely be attributed to a frequency modulation resulting from the driven micromotion of the ions in the trap. For the fitting of the two-photon line shapes, good agreement with theory was obtained for a width of the $24\,874_{5/2}$–$49\,960_{7/2}$ resonance which is four times bigger than the width of the $24\,874_{5/2}$ resonance. The resulting linewidths for excitation with co- and counterpropagating laser beams are 95 and 66 MHz, respectively.

Using the pulsed picosecond Ti:sapphire laser for the second excitation step results in weak fluorescence signals which did not allow us to identify the excitation of higher-lying

states. The broad spectrum emitted by this laser excites several resonances from low-lying metastable levels simultaneously.

VII. CONCLUSION

In conclusion, we have demonstrated two-photon excitation of Th$^+$ through the intermediate state at $24\,874_{5/2}$. In order to maximize the population of excited states we investigated collisional quenching of metastable states with different buffer gases and repumping with additional lasers. In continuous excitation with two diode lasers, we have shown the efficient two-photon excitation of a highly excited state in this complex level-structure. This sets the ground for a comprehensive investigation of the electronic level structure of Th$^+$ in the energy range of the ^{229}Th isomeric state [23] and for the search for a resonant two-photon electronic bridge excitation of the ^{229}Th nucleus [8] over the wide present uncertainty range for the transition energy. For this we plan to use the third harmonic of a pulsed Ti:sapphire laser with a linewidth in the GHz range in combination with synchronized 402-nm ECDL pulses. A comparison of the fluorescence signals observed with ^{229}Th$^+$ and with ^{232}Th$^+$ shall permit the unambiguous identification of the signature of the unique nuclear structure of ^{229}Th.

[1] B. R. Beck, J. A. Becker, P. Beiersdorfer, G. V. Brown, K. J. Moody, J. B. Wilhelmy, F. S. Porter, C. A. Kilbourne, and R. L. Kelley, Phys. Rev. Lett. **98**, 142501 (2007).

[2] B. R. Beck, J. A. Becker, P. Beiersdorfer, G. V. Brown, K. J. Moody, C. Y. Wu, J. B. Wilhelmy, F. S. Porter, C. A. Kilbourne, and R. L. Kelley, Lawrence Livermore National Laboratory, Internal Report LLNL-PROC-415170, 2009.

[3] S. Matinyan, Phys. Rep. **298**, 199 (1998).

[4] E. V. Tkalya, Phys. Usp. **46**, 315 (2003).

[5] E. Peik and Chr. Tamm, Europhys. Lett. **61**, 181 (2003).

[6] C. J. Campbell, A. G. Radnaev, and A. Kuzmich, Phys. Rev. Lett. **106**, 223001 (2011).

[7] W. G. Rellergert, D. DeMille, R. R. Greco, M. P. Hehlen, J. R. Torgerson, and E. R. Hudson, Phys. Rev. Lett. **104**, 200802 (2010).

[8] S. G. Porsev, V. V. Flambaum, E. Peik, and C. Tamm, Phys. Rev. Lett. **105**, 182501 (2010).

[9] R. Zalubas and C. H. Corliss, J. Res. Natl. Bur. Stand., Sect. A **78**, 163 (1974), [http://nistdigitalarchives.contentdm.oclc.org/cdm/ref/collection/p13011coll6/id/63425].

[10] B. A. Palmer and R. Engleman, Jr., *Atlas of the Thorium Spectrum* (Los Alamos National Laboratory, Los Alamos, 1983).

[11] V. A. Dzuba and V. V. Flambaum, Phys. Rev. Lett. **104**, 213002 (2010).

[12] W. Kälber, J. Rink, K. Bekk, W. Faubel, S. Göring, G. Meisel, H. Rebel, and R. C. Thompson, Z. Phys. A **334**, 103 (1989).

[13] W. Kälber, G. Meisel, J. Rink, and R. C. Thompson, J. Mod. Opt. **39**, 335 (1992).

[14] H. Nilsson, Z. G. Zhang, H. Lundberg, S. Johansson, and B. Nordström, Astron. Astrophys. **382**, 368 (2002).

[15] W. Paul, Rev. Mod. Phys. **62**, 531 (1990).

[16] K. Zimmermann, M. V. Okhapkin, O. A. Herrera-Sancho, and E. Peik, Appl. Phys. B, doi:10.1007/s00340-012-4884-1.

[17] L. R. Churchill, M. V. DePalatis, and M. S. Chapman, Phys. Rev. A **83**, 012710 (2011).

[18] B. Arcimowicz, A. Huss, S. Roth, N. Jaritz, D. Messnarz, G. H. Guthöhrlein, H. Jäger, and L. Windholz, Eur. Phys. J. D **13**, 187 (2001).

[19] A. Krzykowski and D. Stefańska, J. Phys. B **41**, 055001 (2008).

[20] H. Simonsen, T. Worm, P. Jessen, and O. Poulsen, Phys. Scr. **38**, 370 (1998).

[21] A. A. Madej and J. D. Sankey, Phys. Rev. A **41**, 2621 (1990).

[22] M. Knoop, M. Vedel, and F. Vedel, Phys. Rev. A **58**, 264 (1998).

[23] S. G. Porsev and V. V. Flambaum, Phys. Rev. A **81**, 042516 (2010).

[24] J. E. Bjorkholm and P. F. Liao, Phys. Rev. A **14**, 751 (1976).